

Original Article

Research findings working with the *p53* and *Rb1* targeted osteosarcoma mouse model

Yaojuan Lu¹, Steven Gitelis², Guanghua Lei^{1,3}, Ming Ding¹, Carl Maki¹, Ranim R Mira¹, Qiping Zheng^{1,4}

Departments of ¹Anatomy and Cell Biology, ²Orthopaedic Surgery, Rush University Medical Center, Chicago, IL 60612, USA; ³Department of Orthopaedic Surgery, Xiangya Hospital, Central South University, Changsha 410008, China; ⁴Department of Hematology and Hematological Laboratory Science, School of Medical Science and Laboratory Medicine, Jiangsu University, Zhenjiang 212013, China

Received February 19, 2014; Accepted March 20, 2014; Epub May 26, 2014; Published June 1, 2014

Abstract: Osteosarcoma (OS) is the most common bone cancer in children and young adults. The etiology of osteosarcoma is currently unknown. Besides the predominant osteoblasts, the presence of cartilage forming chondrocytes within its tumor tissues suggests a role of chondrogenesis in osteosarcoma development. Runx2 is a master transcription factor both for osteoblast differentiation and for chondrocyte maturation. Interestingly, RUNX2 has been shown to directly interact with *p53* and *Rb1*, two genes essential for osteosarcoma development in mice. However the in vivo relevance of Runx2 during osteosarcoma progression has not been elucidated. We have recently shown that targeting Runx2 expression in hypertrophic chondrocytes delays chondrocyte maturation. It has also been shown that osteoblast-specific deletion of *p53* and *Rb1* genes developed osteosarcoma in mice. Here, we report our recent research findings using these osteosarcoma mouse models as well as human osteosarcoma tissues. We have detected high-level RUNX2 expression in human osteoblastic osteosarcoma, while chondroblastic osteosarcoma is predominant with chondroid matrix. To minimize the effect of strain difference, we have backcrossed osterix-Cre mice onto congenic FVB/N genetic background. We also detected low-GC content (36%) in sequence around the floxed *Rb1* gene and demonstrated that addition of BSA into the reaction system increases the efficiency of PCR genotyping of floxed *Rb1* gene. Finally, we successfully generated multiple osteosarcoma mouse models with or without Runx2 transgenic background. These mice showed heterogeneous osteosarcoma phenotypes and marker gene expression. Characterization of these mice will facilitate understanding the role of Runx2 in osteosarcoma pathogenesis and possibly, for osteosarcoma treatment.

Keywords: Osteosarcoma mouse model, *p53* and *Rb1*, Runx2, BSA, PCR genotyping

Introduction

Osteosarcoma (OS) is the most common pediatric bone cancer. It is also the leading cause of cancer death in children and young adults [1]. The cause of osteosarcoma is currently unknown. Previous studies have suggested the importance of osteoblast activity in its tumorigenesis, as the characteristic feature of osteosarcoma is abnormal bone formation (osteoid matrix) in its tumor tissue, while the predominant cell type within osteosarcoma is the osteoblast [2]. However, there is no evidence that osteoblast, once differentiated from osteoprogenitor cells, can revert to primitive or malignant cells [3]. Notably, many other cell types such as chondrocytes, adipocytes, and fibro-

blasts also appear within osteosarcoma. The fact that chondroid phenotype due to cartilage formation has been reported not only in osteosarcoma cell line, but also in mouse and human osteosarcoma tissues, suggests a role of chondrogenesis or endochondral ossification in osteosarcoma development [4, 5].

Chondrocyte hypertrophy or maturation is a critical late stage of endochondral ossification linking bone and cartilage development. We surmise that chondrocyte maturation may share common mechanisms of angiogenesis and apoptosis with bone cancer formation. Runx2, the Runt domain transcription factor, is essential both for osteoblast differentiation and for chondrocyte maturation [6-9].

Interestingly, Runx2 has previously been linked to many human cancers and is critical for bone metastases in prostate and breast cancers [10]. High-level RUNX2 expression was also detected not only in developing human bones but also in various bone tumors, including osteosarcoma [11]. Given its dual functions during cancer formation, Runx2 may contribute to osteosarcoma tumorigenesis via its oncogenic potential and deregulation of its tumor suppressor function [12, 13]. However, the *in vivo* relevance of Runx2 with osteosarcoma progression remains largely unknown.

We have recently shown that targeting Runx2 expression in mice using the hypertrophic chondrocyte-specific collagen type X gene (*Col10a1*) control elements leads to delayed chondrocyte maturation and reduced chondrocyte apoptosis [14]. Increased expression of anti-apoptotic genes, such as *Bcl-2*, *Opn* and *Sox9*, was also detected in the transgenic mice, suggesting the oncogenic property of Runx2 [14, 15]. Meanwhile, it was previously reported that mice with restricted deletion of *p53* and *Rb1* genes using osterix-Cre mice reproduce many features of human osteosarcoma [4]. Moreover, Runx2 has been shown to directly interact with *p53* and *Rb1* genes [16, 17]. This allows us to determine the *in vivo* effects of Runx2 on osteosarcoma progression by crossing the osteosarcoma mouse model onto the Runx2 transgenic background. In this manuscript, we report detection of chondroid matrix and high-level RUNX2 expression in human chondroblastic and osteoblastic osteosarcoma respectively. We also report the findings while delineating the role of Runx2 regulated chondrocyte maturation during osteosarcoma development using above osteosarcoma and transgenic mouse models [4, 14]. We have backcrossed osterix-Cre mice from C57BL/6 onto congenic FVB/N genetic background so as to minimize the influence of mouse genetic background on osteosarcoma phenotype. We have demonstrated that addition of BSA (Bovine serum albumin) can overcome the low efficiency of PCR-genotyping of *floxed Rb1* gene due to its low-GC content. We successfully generated multiple osteosarcoma mouse models with or without a Runx2 transgenic background. These mice showed heterogeneous osteosarcoma phenotypes as to the tumor latency and severity. High-level Runx2 expression was also detected in tumor tissue.

Materials and methods

Collection of human osteosarcoma tissue samples

After informed consent, surgically removed fresh tumor samples were collected from osteosarcoma patients at the Department of Orthopaedic Surgery and the Department of Pathology, Rush University Medical Center. Preoperational chemotherapy, biopsy and pathological diagnosis were conducted by experienced orthopaedic oncologist and pathologist. The tumor samples were subjected to histology, immunohistochemical staining, RNA extraction and expression analysis as described below. The human studies were approved by the Institutional Review Board (IRB) of Rush University Medical Center (ORA#: 08091504-IRB01).

Mouse models

This study involves following four mouse models. The *Col10a1-Runx2* (*Tg-Runx2*) transgenic mice have recently been described [14]. These mice are on a FVB/N genetic background and exhibit delayed ossification, chondrocyte maturation and reduced apoptosis [14]. The original *p53* floxed heterozygous mice (01XC2, FVB.129-Trp53tm1Brn) and the *Rb1* floxed homozygous mice (01XC1, FVB;129-Rb1tm2Brn) were obtained from the National Cancer Institute (NCI) Mouse Repository with appropriate Material Transfer Agreement (MTA) [18, 19]. These mice are on a FVB/N and 129 genetic backgrounds. The *Osx-1-GFP::Cre* mice were purchased from the Jackson laboratory (006361, B6.Cg-Tg(Sp7-tTA,tetO-EGFP/cre)1Amc/J [20]. These mice are on a C57BL/6 genetic background.

Mouse breeding

Sex-matured (8-10 weeks' age) *Osx-1-GFP::Cre* mice on C57BL/6 genetic background were backcrossed with wild-type FVB/N mice to obtain congenic FVB/N strain of mice. The floxed *p53* heterozygous mice (*p53fl/+*) were crossed with the floxed *Rb1* homozygous mice (*Rb1fl/fl*) so as to generate floxed *p53* and floxed *Rb1* double homozygous mice (*p53fl/fl/Rb1fl/fl*). These double homozygous mice were crossed with the congenic *Osx-1-GFP::Cre* mice and subsequently bred with the *Tg-Runx2* mice so as to generate osteosarcoma mouse models

Runx2 and mouse osteosarcoma

Table 1. Primers for PCR-genotyping of Mice

Mice Type	Gene RefSeqID	Sense Primer (5'-3')	Antisense Primer (5'-3')	Amplicon
<i>Tg-Runx2</i>	NM_001145920	CTTCCCAAAGCCAGAGTGGAC	TGTCGTCATCGTCTTTGTAGC	300-bp
<i>Osx-Cre</i>	NC_005856.1	TGCAACGAGTGATGAGTTTCG	CATGTTTAGCTGGCCCAAATGT	250-bp
<i>P53/floxed</i>	NM_011640.3	CACAAAAACAGTTAAACCCAG	AGCACATAGGAGGCAGAGAC	288/370-bp
<i>Rb1/floxed</i>	NM_009029.2	GGCGTGTGCCATCAATG	AACTCAAGGGAGACCTG	650/700-bp
<i>Rb1/floxed</i>	NM_009029.2	GGAATTCGGCGTGTGCCATCAATG	AGCTCTCAAGAGCTCAGACTCATGG	247/295-bp

Runx2: Runt-related transcription factor 2; *Cre*: Cre recombinase; *p53*: Transformation-related protein 53; *Rb1*: Retinoblastoma 1.

with or without the *Runx2* transgenic background. Detailed breeding strategy was described in the Result section. All the mouse studies were approved by the animal care and oversight committee at Rush University Medical Center.

PCR genotyping and target gene sequence analysis

The offspring of multiple breeding pairs of mice were weaned at the age of 3-4 weeks. Genomic DNAs from mouse tail tissues (~0.5 cm long) were extracted by traditional phenol/chloroform method. The DNAs were then used as templates for subsequent PCR genotyping using gene- or tag sequence-specific primers. Specifically, the *Col10a1-Runx2* transgenic mice were PCR-genotyped using *Runx2*- and *Flag-tag* sequence-specific primers [14]. The *Osx-Cre* mice were genotyped using *Cre*-specific primers. The primers for PCR-genotyping of floxed *p53* or *Rb1* gene (two pairs) were synthesized according to NCI database and literatures [18-22]. The gene reference number, the primer sequence, and the amplicon size are all summarized in **Table 1**. The GC content of the sequences used for PCR genotyping was calculated using the OligoCalc, an online oligonucleotide property calculator available at <http://basic.northwestern.edu/biotools/OligoCalc.html> [23].

Osteosarcoma phenotypes—histology and IHC analysis

After weaning and PCR genotyping, mice that are expected to develop osteosarcoma are frequently examined. Mice suffering from fast growing osteosarcoma (usually at upper or lower jaw and snout) were euthanized under anesthesia. For histological analysis, a portion of the mouse (as well as surgically removed human) osteosarcoma tissues were collected and fixed in 10% formalin, followed by dehydra-

tion, paraffin embedding, sectioning, and subjected to standard Hematoxylin & Eosin staining. For immunohistochemical (IHC) analysis, pretreated human and mouse tumor sections were incubated with anti-Runx2 (M-70, sc-10758, Santa Cruz, CA) antibody as previously described [14]. The concentration for primary anti-Runx2 antibody was at 1:50 dilution and non-immune mouse IgG was used as a negative control. The biotinylated anti-rabbit IgG (Santa Cruz, CA) was used as a secondary antibody. The ABC kit (Elite PK-6200 Universal, VECTOR laboratories, Burlingame, CA) was used for detection and slides were counterstained with nuclear fast red (Poly Scientific R&D Corp., NY). Microscopic analysis was using the Nikon Eclipse 80i (Nikon Instruments Inc., Melville, NY USA) and the Qcapture Suite software (version, 2.95.0, Quantitative Imaging Corp., USA).

Osteosarcoma phenotypes—gene expression analysis

Total RNAs from fresh mouse osteosarcoma tissue and mouse limbs were isolated using Trizol reagents (Invitrogen, Carlsbad, CA) and subsequently reverse transcribed using Superscript III reverse transcriptase (Invitrogen, Carlsbad, CA). The cDNA template was used for qRT-PCR to examine following gene expression using the MyiQ Single Color Real-Time PCR Detection System and SYBR Green master mix (Bio-Rad, Hercules, CA). Total RNAs from mouse limbs that were previously extracted were used as controls [14]. The genes examined include *Bax*, *Bcl-2*, *Runx2*, and the endogenous control gene *Gapdh* for normalization of the RNA quality and quantity. The sequences of the primers used for qRT-PCR were as previously listed [14]. Relative mRNA level was automatically analyzed by the manufacturer provided MyiQ Optical System Software. The mean threshold cycle number (CT values) of target genes was normalized to *Gapdh* and calculated using

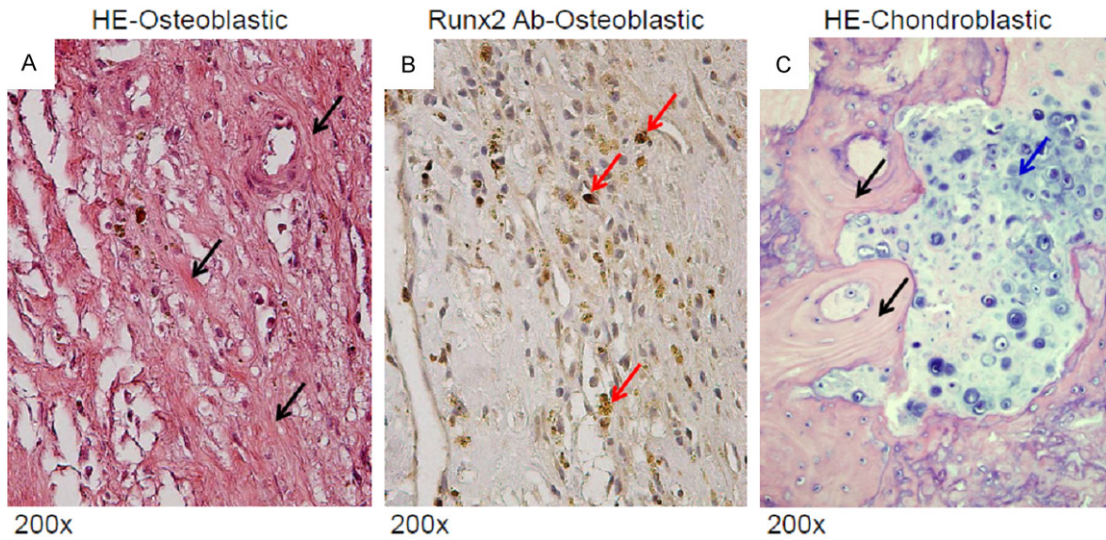


Figure 1. Human osteoblastic and chondroblastic osteosarcoma. A: H&E staining of a representative osteoblastic osteosarcoma showed osteoid deposition and bone matrix to form a lace-like pattern (black arrows) with scattered osteoblast-like cells. B: IHC analysis using Runx2 antibody detected Runx2 expression in a variety of osteoblasts within osteoblastic osteosarcoma tissue (red arrows). C: H&E staining of a representative chondroblastic osteosarcoma showed predominantly chondroid matrix with high grade hyaline cartilage (blue arrow). The lace-like pattern indicating osteoid production was also observed (black arrows).

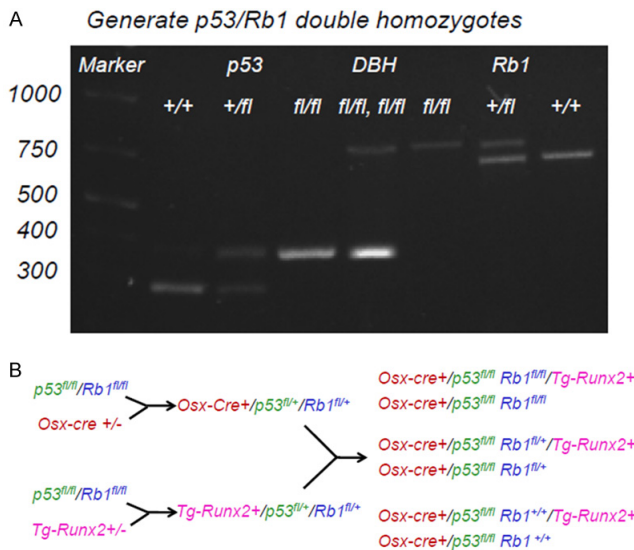


Figure 2. Strategies generating osteosarcoma mouse models. A: Illustrated is PCR genotyping result of floxed p53 and Rb1 genes showing corresponding p53 or Rb1 wild-type (+/+), heterozygous (+/fl), and homozygous (fl/fl) mice. DBH: double homozygous mice. B: Illustrated is the breeding chart showing how to use p53 and Rb1 double homozygous mice to generate Cre- or Runx2- triple heterozygotes, and subsequently, multiple osteosarcoma mouse models with or without the Tg-Runx2 background as partially listed.

templates and the relative mRNA level was compared between osteosarcoma mouse models. $p < 0.05$ was considered statistically significant fold change of mRNA level between samples.

Results

Human osteoblastic and chondroblastic osteosarcoma

We have collected tumor tissues from ~20 osteosarcoma patients with surgery. Most of the tumor tissues were from left or right femurs or tibias (either proximal or distal). Some tumors were from the pelvis or foot. These tumor tissues show a variety of pathological features of osteoblastic, chondroblastic, fibroblastic or pleomorphic sarcoma of bone. Illustrated is H&E staining of a representative tumor sample showing characteristics of osteoblastic osteosarcoma, i.e. production of osteoid and bone matrix in a lacy pattern that is incorporated with the osteoblast-like malignant cells (Figure 1A). We have performed IHC analysis using anti-Runx2 antibody and the result showed that RUNX2 is expressed in malignant cells of osteosarcoma (Figure 1B).

$2^{-\Delta\Delta Ct}$ and student t-test [24, 25]. Data is collected from multiple runs with duplicate

Runx2 and mouse osteosarcoma

Table 2. Generation of Congenic *Osx-Cre* Mice

Mice For backcross	Genome (F1/Gen 1)	Genome (Gen 2)	Genome (Gen 3)	Genome (Gen 4)	Genome (Gen 5)	Genome (Gen 6)	Genome (Gen 7)	Genome (Gen 8)	Genome (Gen 9)	Genome (Gen10)
<i>Osx-Cre</i> (C57Bl/6)	50%	25%	12.5%	6.25%	3.12%	1.56%	0.78%	0.39%	0.19%	0.10%
Wild-type (FVB/N)	50%	75%	87.5%	93.75%	96.88%	98.44%	99.22%	99.61%	99.81%	99.90%

Table 3. Summary of osteosarcoma mouse models

mOS No.	Gender	<i>Osx-Cre</i>	<i>Tg-Runx2</i>	Floxed <i>p53</i>	Floxed <i>Rb1</i>	Latency (M)	Tumor site
1	F	+	-	<i>p53fl/+</i>	<i>Rb1fl/+</i>	5.5	Jaw/snout
2	M	+	-	<i>p53fl/fl</i>	<i>Rb1fl/+</i>	4.4	Lower jaw
3	M	+	-	<i>p53fl/fl</i>	<i>Rb1fl/+</i>	5.7	Lower jaw
4	F	+	-	<i>p53fl/fl</i>	<i>Rb1fl/fl</i>	5.5	Right snout
5	M	+	-	<i>p53fl/fl</i>	<i>Rb1fl/fl</i>	5.3	Right snout
6	M	+	-	<i>p53fl/+</i>	<i>Rb1fl/fl</i>	5.7	Fore limb
7	F	+	-	<i>p53fl/fl</i>	<i>Rb1fl/fl</i>	3.9	Right snout
8	F	+	+	<i>p53fl/fl</i>	<i>Rb1+/+</i>	7.7	Spine
9	F	+	+	<i>p53fl/+</i>	<i>Rb1fl/+</i>	4.5	Lower jaw
10	M	+	+	<i>p53fl/fl</i>	<i>Rb1fl/+</i>	5.1	Left snout
11	M	+	+	<i>p53fl/fl</i>	<i>Rb1fl/fl</i>	5.4	Lower jaw
12	F	+	+	<i>p53fl/fl</i>	<i>Rb1fl/+</i>	1.6	Sarcoma

We also show H&E staining of a representative chondroblastic osteosarcoma. The tumor tissue is predominant with chondroid matrix containing high grade hyaline cartilage, as well as lace-like pattern indicating osteoid production (Figure 1C).

Strategies generating osteosarcoma mouse models

In order to generate osteosarcoma mouse models with or without the *Col10a1-Runx2* transgenic background, we have used a series of breeding strategies to obtain multiple intermediate mouse models. These mouse models include congenic *Osx-Cre* mice in FVB/N genetic background, floxed *p53/Rb1* double homozygous mice (*p53fl/fl/Rb1fl/fl*), and floxed *p53/Rb1* mice on the *Col10a1-Runx2* or *Osx-Cre* transgenic background (Figure 2A). Briefly, we have backcrossed the C57BL/6 *Osx-Cre* mice (donor strain) with wild-type FVB/N mice (receiver strain). After ten generations' backcrossing, we successfully obtained congenic *Osx-Cre* mice in a FVB/N genetic background (Table 2). We then generated floxed *p53* and *Rb1* double homozygous mice (*p53fl/fl, Rb1fl/fl*) by breeding above floxed *p53* heterozygotes (*p53fl/+*) with the floxed *Rb1* homozygotes (*Rb1fl/fl*) as demonstrated by PCR genotyping (Figure 2B). These *p53* and *Rb1* double homo-

zygotes were bred with congenic *Osx-Cre* or *Tg-Runx2* mice to generate *p53fl/+*, *Rb1fl/+*, *Osx-Cre* and *p53fl/+*, *Rb1fl/+*, *Tg-Runx2* triple heterozygous mice. Further breeding of these triple heterozygotes were conducted to generate multiple osteosarcoma mouse models as described below.

Osteosarcoma mouse models and *Tg-Runx2* background

We have set up multiple breeding pairs using *Osx-Cre* (*p53fl/+*, *Rb1fl/+*) and *Tg-Runx2* (*p53fl/+*, *Rb1fl/+*) triple heterozygotes. Mouse models that were genotyped and developed osteosarcoma were summarized in Table 3. Generally, mice with osteoblast restricted deletion of *p53* and/or *Rb1* genes (*p53fl/fl, Rb1fl/fl, Osx-Cre+*) without having the *Tg-Runx2* genetic background consistently developed osteosarcoma as previously established [4]. These mice show similar tumor latency and site distribution (jaw and snout) depending on their genotyping. Meanwhile, mouse models with similar genotypes but on a *Tg-Runx2* genetic background (*p53fl/fl, Rb1fl/fl, Osx-Cre+*, *Tg-Runx2*) showed heterogeneous osteosarcoma phenotypes as to tumor latency types, and location. In addition to the jaw and snout, some of the mouse models also developed spine tumors and sarcoma or adipoma in connective tissue of inner organs

Runx2 and mouse osteosarcoma

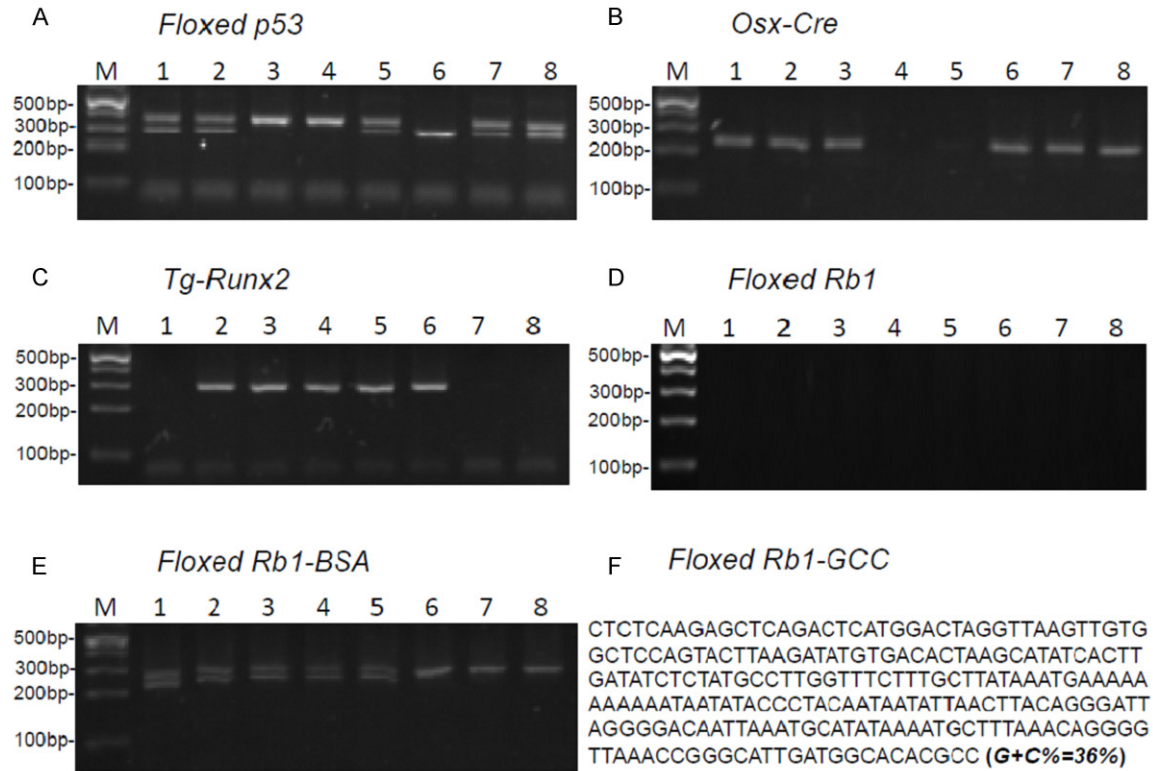


Figure 3. PCR genotyping of osteosarcoma mouse models. A: The genotyping result showed that mice 1, 2, 5, 7, and 8 are floxed *p53* heterozygotes, mice 3 and 4 are homozygotes, while mouse No. 6 is wild-type. B: Genotyping using *Cre*-specific primers identified mice 1, 2, 3, 6, 7, and 8 as *Osx-Cre* positive, while mice 4 and 5 are *Osx-Cre* negative. C: PCR using *Runx2*- and *Flag*-specific primers identified mice 2-6 as *Runx2* transgenic while mice 1, 7, and 8 did not contain *Runx2* transgene. D: PCR using *Rb1*-specific primers without addition of BSA failed to detect floxed *Rb1* gene products. E: Addition of BSA into the PCR reaction system successfully identified mice 1-5 as floxed *Rb1* heterozygotes, while mice 6-8 are floxed *Rb1* homozygotes. F: The GC content of the floxed *Rb1* PCR products is 36% as calculated by the OligoCalc program [23]. M: DNA marker; GCC: G+C% content.

at the early stage of ~1.5 months (No. 8 and 12 in **Table 3**).

BSA in PCR genotyping of floxed *Rb1* gene

PCR genotyping was performed using combined tag (*Cre*- and *Flag*-) and gene (*p53*, *Rb1*, *Osx1*, and *Runx2*) specific primers (**Table 1**) and NCI and literature suggested PCR conditions [18-22]. Interestingly, the PCR genotyping was successful for floxed *p53*, *Osx-Cre* and *Tg-Runx2* transgene (**Figure 3A-C**), but not floxed *Rb1* gene, as no PCR product was shown using the *Rb1*-specific primers (**Figure 3D**). The PCR genotyping was not successful either when we tried to optimize the cycling condition, use PCR additives (such as DMSO, glycerol and formamide), or even design new primer pairs for PCR (data not shown). However, when BSA (0.16 mg/ml) was added to the PCR system, we successfully obtained the PCR product flanking

the floxed *Rb1* gene (**Figure 3E**). To identify the potential reasons causing the discrepancy of PCR genotyping, we calculated the GC content of their PCR products using the OligoCalc program [23]. The results showed that the GC content of the *Osx-Cre*, floxed *p53*, and *Tg-Runx2* amplicons are 50%, 48%, and 52% respectively (data not shown), while the GC content of the floxed *Rb1* PCR products is only 36% (**Figure 3F**).

HE staining and *Runx2* expression in mouse osteosarcoma

To characterize above osteosarcoma mouse models, we performed H&E staining of mice numbered 1, 4, 9, and 11. Mice No. 1 and 9 were floxed *p53* and *Rb1* gene double heterozygotes, while mice No. 4 and 11 were floxed *p53* and *Rb1* double homozygotes. All these mice were *Cre* positive with mice No. 9 and 11 hav-

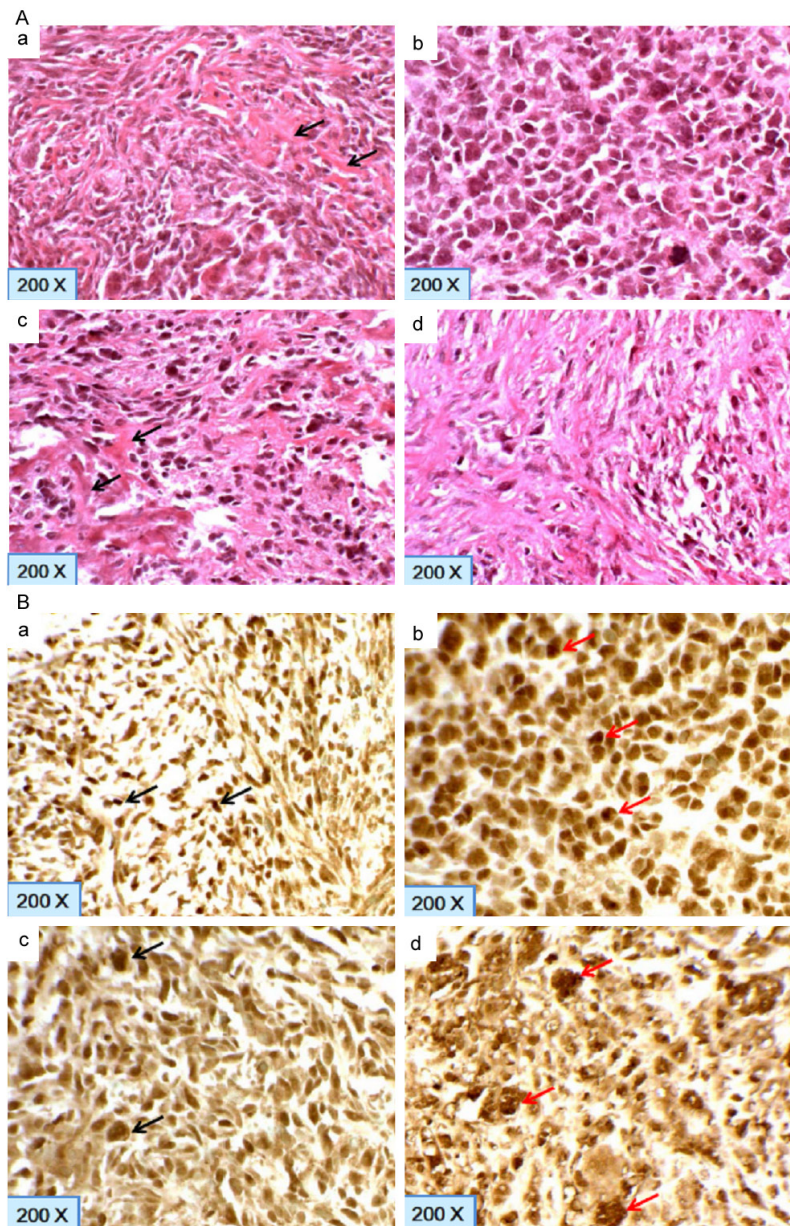


Figure 4. H&E and IHC analysis of mouse osteosarcoma. (A) H&E staining of *Osx-Cre* positive, and floxed *p53/Rb1* double heterozygotes (a, mouse No. 1) or homozygotes (c, mouse No. 4) without *Tg-Runx2* transgene showed typical pathological features of osteoblastic osteosarcoma, including osteoid production and ill-shaped osteoblasts (black arrows). Similar but more irregular osteoblast-like cells and nuclear pleomorphism were observed in *Osx-Cre* positive, and floxed *p53/Rb1* double heterozygotes (b, mouse No. 9) or homozygotes (d, mouse No. 11) that contain a *Runx2* transgene. (B) IHC analysis of above mice No. 1 (a) and No. 4 (c) detected clear Runx2 expression in scattered and ill-shaped osteoblasts (black arrows). Stronger brown staining indicating elevated Runx2 expression was observed in malignant osteoblasts and pleomorphic nuclei of mice No. 9 (b) and 11 (d).

ing a *Tg-Runx2* genetic background (Table 3). These mice with different genotypes showed typical pathological features of osteosarcoma after HE staining. Specifically, osteoid produc-

tion or bone formation with incorporated malignant osteoblasts was observed in *Osx-Cre* mice with floxed *p53/Rb1* double heterozygotes and homozygotes (Figure 4Aa, 4Ac, mice No. 1 and 4). Similar histological manifestation with more malignant cells and nuclear pleomorphism was observed in mice with the same genotypes but have a *Tg-Runx2* genetic background (Figure 4Ab, 4Ad, mice No. 9 and 11). To study the correlation of Runx2 with mouse osteosarcoma development, we performed IHC analysis using Runx2 antibody on osteosarcoma mouse models with or without the *Tg-Runx2* genetic background. The result showed that Runx2 is clearly expressed in osteosarcoma tissues without *Tg-Runx2* background (Figure 4Ba, 4Bc, mice No. 1 and 4), while elevated Runx2 expression as shown by stronger brown staining signal was observed in malignant osteoblasts and pleomorphic nuclei of osteosarcoma tissues with *Tg-Runx2* genetic background (Figure 4Bb, 4Bd, mice No. 9 and 11).

Marker gene expression in selective mouse osteosarcoma

We have performed expression analysis of marker genes *Bax*, *Bcl-2*, and *Runx2* in selective osteosarcoma tissues by qRT-PCR. As illustrated in

Figure 5, we detected significantly increased level of Runx2 expression in tumor tissues of mice with (*mOS-1*, $p=0.048$) or without (*mOS-8*, $p=0.012$) *Tg-Runx2* background compared

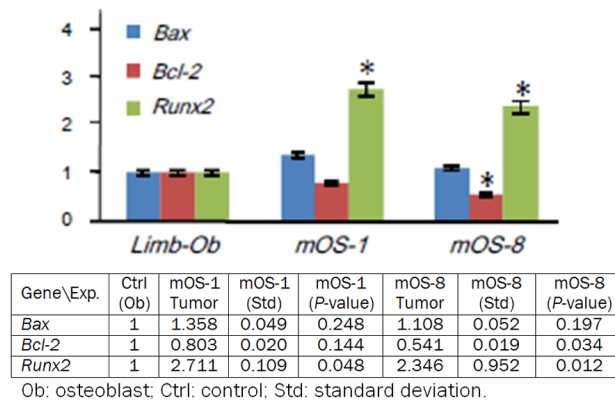


Figure 5. Expression analysis of marker genes in mouse osteosarcoma. qRT-PCR was performed to examine *Bax*, *Bcl-2*, and *Runx2* gene expression in osteosarcoma tissues of mice No. 1 (*mOS-1*) and No. 8 (*mOS-8*). As illustrated, *Runx2* is significantly increased in tumor tissues of *mOS-1*, ($p=0.048$) and *mOS-8* ($p=0.012$) compared to mouse limb osteoblasts. Both *mOS-1* and *mOS-8* showed increased *Bax* expression, but not statistically significant. *Bcl-2* was decreased both in *mOS-1* and in *mOS-8*, but only *mOS-8* showed statistical significance ($p=0.034$). Ob: osteoblast; OS: osteosarcoma.

to mouse limb osteoblasts. Increased *Bax* but decreased *Bcl-2* expression was detected both in *mOS-1* and in *mOS-8* tumor tissues compared to limb osteoblasts. However, only the decreased *Bcl-2* expression in *mOS-8* showed statistical significance ($p=0.034$). Meanwhile, analysis of other mouse tumors only detected heterogeneous expression of these marker genes (data not shown).

Discussion

Established mouse models for osteosarcoma genetics studies

Currently, the etiology of human osteosarcoma is largely unknown and even less is known as to the factors that govern the in vivo osteosarcoma progression and metastasis. Previously, many efforts have been focused on characterization of mouse or human osteosarcoma cell lines in vitro due to shortage of suitable animal models that mimic human osteosarcoma [26]. However, recent mouse genetic studies have shown that osteoblast-specific deletion of *p53* and *Rb1* using the *Osx-Cre* mice results in symptoms mimic human osteosarcoma. These genetically engineered mice develop short tumor latency with many defining features of human osteosarcoma, and thus, provide a valuable platform for addressing the molecular genetics of osteosarcoma [4]. Given the close

correlation of *Runx2* with bone and cancer formation [6, 7, 10-13, 27-30], we investigated the in vivo relevance of *Runx2* upon osteosarcoma development using this established osteosarcoma mouse model and the *Col10a1-Runx2* transgenic mice that showed delayed chondrocyte maturation [14]. In this manuscript, we have shown multiple original findings while delineating the role of *Runx2* regulated chondrocyte maturation during osteosarcoma progression.

Congenic *Osx-Cre* mice in FVB/N genetic background

We notice that the previously established osteosarcoma mouse models, the *Osx-Cre* mice, the floxed *p53* and *Rb1* mice were all on a C57BL/6 genetic background. In our study, while the *Osx-Cre* mice are still on a C57BL/6 background, all other *Col10a1-Runx2* transgenic mice, the floxed *p53* and *Rb1* mice from the NCI mouse repository were on a FVB/N mixed genetic background. To minimize the influence of mouse strain difference on tumor phenotypes, we have backcrossed *Osx-Cre* mice (donor strain) with wild-type FVB/N mice (recipient strain) for ten generations. Theoretically, each generation of *Osx-Cre* mice eliminated 50% genome content of C57BL/6 strain. After ten generations' backcrossing, more than 99.9% of the donor's genome was eliminated, and thus, we successfully generated congenic *Osx-Cre* mice from C57BL/6 to a FVB/N genetic background. These mice may serve better for osteosarcoma translational research, as previous studies have shown that mice on FVB background have much shorter tumor latency compared to C57BL/6 background [31, 32].

BSA application in PCR genotyping

The multiple mouse models in this study rely largely on accurate and efficient genotypic analysis. We successfully conducted PCR genotyping for *Osx-Cre*, floxed *p53*, and *Tg-Runx2* mice (Figure 3A-C). Interestingly, PCR genotyping frequently failed to detect floxed *Rb1* gene product which led to false negative result (Figure 3D). It would not succeed simply by changing the PCR cycling condition (annealing temperature) and parameters (concentration of $MgCl_2$). We also tried different pairs of primers for floxed *Rb1* gene and add known PCR addi-

tives, such as DMSO (Dimethyl Sulfoxide), formamide or glycerol, into the reaction system [33, 34], however, no PCR product was amplified (data not shown). Given its ability to stabilize enzyme activity, BSA has generally been used as an additive in restriction enzyme digestions. BSA has also been used as a PCR additive for templates that contain potential inhibitors such as trace of phenol compounds during genome DNA extraction [35]. Indeed, we successfully obtained PCR product for floxed *Rb1* using both primer pairs (**Figure 3E** and data not shown). It is well accepted that high GC-rich DNA samples (GC content >60) usually cause limited yield and poor specificity of the reaction due to secondary structure formed by the PCR product. We, therefore, calculated the GC content of the *Osx-Cre*, floxed *p53*, *Rb1*, and *Tg-Runx2* amplicons. Surprisingly, only the floxed *Rb1* PCR product shows a GC content as low as 36% (**Figure 3F**). This finding at least partially explains the inefficiency of PCR genotyping of floxed *Rb1*, as previous studies have demonstrated the low efficiency of PCR with DNA templates that contain too low (<40%) or too high (>60%) GC content [36].

Runx2 and marker gene expression in osteosarcoma

Runx2 is a Runt domain transcription factor that regulates both osteoblast differentiation and chondrocyte maturation [6-9]. Runx2 has also been strongly linked to many human cancers [37]. As to osteosarcoma, we have shown that RUNX2 is highly expressed in osteoblast-like cells in human osteosarcoma tissues (**Figure 1B**). This corresponds well with previous studies which have shown that RUNX2 is expressed both in developing human bones and in bone tumors [11], while increased RUNX2 DNA copy number and elevated RUNX2 expression were also detected in osteosarcoma [12, 38]. It was recently reported that WWOX, a tumor suppressor that is decreased in most human tumors, associates with RUNX2 and suppresses its transcriptional activity in osteoblasts and in cancer cells [39]. Intriguingly, Runx2 has been shown to interact with *p53* and *Rb1*, two genes that are responsible for osteosarcoma development in mice [4, 16, 17].

In our study, we intended to characterize the *in vivo* function of Runx2 during osteosarcoma progression by crossing the established *p53/*

Rb1 deleted osteosarcoma mouse model onto the *Col10a1-Runx2* transgenic background [4, 14]. We successfully generated multiple mouse models that developed osteosarcoma as expected (**Table 3**). These mouse osteosarcoma display a variety of histopathological features as previously described [4, 40]. We have shown that Runx2 is expressed in osteosarcoma tissues without *Tg-Runx2* background (**Figure 4Ba, 4Bc**). Interestingly, we detected stronger immunostaining signal indicating more Runx2 expression in tissues of osteosarcoma mice with the same genotypes but has an extra *Tg-Runx2* background (**Figure 4Bb, 4Bd**). We also detected significantly increased *Runx2* expression in some osteosarcoma tissues compared to limb osteoblast cells by qRT-PCR analysis (**Figure 5**), while significantly decreased *Bcl-2* expression was detected in an osteosarcoma mouse with the *Tg-Runx2* background. However, due to the limited number of osteosarcoma mice we obtained, these observations need further investigation. Interestingly, we observed one mouse with *Runx2* transgenic background (*mOS-12*, **Table 3**) developed sarcomas or adipomas within two months. However, how Runx2 contributes to osteosarcoma tumorigenesis in these mice is not clear yet. Further characterization of the tumor phenotypes of more osteosarcoma mice with or without the *Tg-Runx2* background will facilitate understanding the role of Runx2 in osteosarcoma pathogenesis and, possibly identification of novel therapeutic targets for osteosarcoma treatment.

Acknowledgements

We are grateful to Drs. Rick Sumner, Meghan Moran, and Mr. David Karwo for histological help on transgenic mice at the Rush Histology Core. This work was supported by the American Cancer Society-Illinois Division (#254598, Q.Z., S.G., C.M.) and the National Cancer Institute (NCI/NIH) (R21CA161461, Q.Z., S.G.).

Disclosure of conflict of interest

All authors have no conflict of interest.

Address correspondence to: Dr. Qiping Zheng, Department of Anatomy and Cell Biology, Rush University Medical Center, Chicago, IL 60612, USA. E-mail: qiping_zheng@rush.edu

References

- [1] Kansara M, Thomas DM. Molecular pathogenesis of osteosarcoma. *DNA Cell Biol* 2007; 26: 1-18. Review.
- [2] Bertoni F, Bacchini P. Classification of bone tumors. *Eur J Radiol* 1998; 27 Suppl 1: S74-6.
- [3] Klein MJ, Siegal GP. osteosarcoma: anatomic and histologic variants. *Am J Clin Pathol* 2006; 125: 555-81.
- [4] Walkley CR, Qudsi R, Sankaran VG, Perry JA, Gostissa M, Roth SI, Rodda SJ, Snay E, Dunning P, Fahey FH, Alt FW, McMahon AP, Orkin SH. Conditional mouse osteosarcoma, dependent on p53 loss and potentiated by loss of Rb, mimics the human disease. *Genes Dev* 2008; 22: 1662-76.
- [5] Nishi T, Kusumi T, Tanaka M, Sato F, Sasaki M, Kudo H, Kijima H. Establishment of transplantable murine osteosarcoma cell line with endochondral ossification. *Anticancer Res* 2008; 28: 1627-31.
- [6] Komori T, Yagi H, Nomura S, Yamaguchi A, Sasaki K, Deguchi K, Shimizu Y, Bronson RT, Gao YH, Inada M, Sato M, Okamoto R, Kitamura Y, Yoshiki S, Kishimoto T. Targeted disruption of *Cbfa1* results in a complete lack of bone formation owing to maturational arrest of osteoblasts. *Cell* 1997; 89: 755-64.
- [7] Otto F, Thornell AP, Crompton T, Denzel A, Gilmour KC, Rosewell IR, Stamp GW, Beddington RS, Mundlos S, Olsen BR, Selby PB, Owen MJ. *Cbfa1*, a candidate gene for cleidocranial dysplasia syndrome, is essential for osteoblast differentiation and bone development. *Cell* 1997; 89: 765-71.
- [8] Inada M, Yasui T, Nomura S, Miyake S, Deguchi K, Himeno M, Sato M, Yamagiwa H, Kimura T, Yasui N, Ochi T, Endo N, Kitamura Y, Kishimoto T, Komori T. Maturational disturbance of chondrocytes in *Cbfa1*-deficient mice. *Dev Dyn* 1999; 214: 279-90.
- [9] Kim IS, Otto F, Zabel B, Mundlos S. Regulation of chondrocyte differentiation by *Cbfa1*. *Mech Dev* 1999; 80: 159-70.
- [10] Pratap J, Imbalzano KM, Underwood JM, Cohet N, Gokul K, Akech J, van Wijnen AJ, Stein JL, Imbalzano AN, Nickerson JA, Lian JB, Stein GS. Ectopic *runx2* expression in mammary epithelial cells disrupts formation of normal acini structure: implications for breast cancer progression. *Cancer Res* 2009; 69: 6807-14.
- [11] Sugawara M, Kato N, Tsuchiya T, Motoyama T. *RUNX2* expression in developing human bones and various bone tumors. *Pathol Int* 2011; 61: 565-71.
- [12] Martin JW, Zielenska M, Stein GS, van Wijnen AJ, Squire JA. The Role of *RUNX2* in Osteosarcoma Oncogenesis. *Sarcoma* 2011; 2011: 282745.
- [13] Zaidi SK, Pande S, Pratap J, Gaur T, Grigoriu S, Ali SA, Stein JL, Lian JB, Van Wijnen AJ, Stein GS. *Runx2* deficiency and defective subnuclear targeting bypass senescence to promote immortalization and tumorigenic potential. *Proc Natl Acad Sci U S A* 2007; 104: 19861-6.
- [14] Ding M, Lu Y, Abbassi S, Li F, Li X, Song Y, Geoffroy V, Im HJ, Zheng Q. Targeting *Runx2* expression in hypertrophic chondrocytes impairs endochondral ossification during early skeletal development. *J Cell Physiol* 2012; 227: 3446-56.
- [15] Cameron ER, Neil JC. The *Runx* genes: lineage-specific oncogenes and tumor suppressors. *Oncogene* 2004; 23: 4308-14. Review.
- [16] Zambetti GP, Horwitz EM, Schipani E. Skeletons in the p53 tumor suppressor closet: genetic evidence that p53 blocks bone differentiation and development. *J Cell Biol* 2006; 172: 795-7. Review.
- [17] Pereira BP, Zhou Y, Gupta A, Leong DT, Aung KZ, Ling L, Pho RW, Galindo M, Salto-Tellez M, Stein GS, Cool SM, van Wijnen AJ, Nathan SS. *Runx2*, p53, and pRB status as diagnostic parameters for deregulation of osteoblast growth and differentiation in a new pre-chemotherapeutic osteosarcoma cell line (OS1). *J Cell Physiol* 2009; 221: 778-88.
- [18] Jonkers J, Meuwissen R, van der Gulden H, Peterse H, van der Valk M, Berns A. Synergistic tumor suppressor activity of *BRCA2* and p53 in a conditional mouse model for breast cancer. *Nat Genet* 2001; 29: 418-25.
- [19] Marino S, Vooijs M, van Der Gulden H, Jonkers J, Berns A. Induction of medulloblastomas in p53-null mutant mice by somatic inactivation of Rb in the external granular layer cells of the cerebellum. *Genes Dev* 2000; 14: 994-1004.
- [20] Rodda SJ, McMahon AP. Distinct roles for Hedgehog and canonical Wnt signaling in specification, differentiation and maintenance of osteoblast progenitors. *Development* 2006; 133: 3231-44.
- [21] Berman SD, Calo E, Landman AS, Danielian PS, Miller ES, West JC, Fonhoue BD, Caron A, Bronson R, Bouxsein ML, Mukherjee S, Lees JA. Metastatic osteosarcoma induced by inactivation of Rb and p53 in the osteoblast lineage. *Proc Natl Acad Sci U S A* 2008; 105: 11851-6.
- [22] Flesken-Nikitin A, Choi KC, Eng JP, Schmidt EN, Nikitin AY. Induction of Carcinogenesis by Concurrent Inactivation of p53 and Rb1 in the Mouse Ovarian Surface Epithelium. *Cancer Res* 2003; 63: 3459-3463.
- [23] Kibbe WA. OligoCalc: an online oligonucleotide properties calculator. *Nucleic Acids Res* 2007; 35: W43-46.

Runx2 and mouse osteosarcoma

- [24] Livak KJ, Schmittgen TD. Analysis of relative gene expression data using real-time quantitative PCR and the 2(-Delta Delta C(T)) Method. *Methods* 2001; 25: 402-8.
- [25] Pfaff MW. A new mathematical model for relative quantification in real-time RT-PCR. *Nucleic Acids Res* 2001; 29: e45.
- [26] Ek ET, Dass CR, Choong PF. Commonly used mouse models of osteosarcoma. *Crit Rev Oncol Hematol* 2006; 60: 1-8.
- [27] Yang J, Zhao L, Tian W, Liao Z, Zheng H, Wang G, Chen K. Correlation of WWOX, RUNX2 VEGFA protein expression in human osteosarcoma. *BMC Med Genomics* 2013; 6: 56.
- [28] van der Deen M, Akech J, Lapointe D, Gupta S, Young DW, Montecino MA, Galindo M, Lian JB, Stein JL, Stein GS, van Wijnen AJ. Genomic promoter occupancy of runt-related transcription factor RUNX2 in osteosarcoma cells identifies genes involved in cell adhesion and motility. *J Biol Chem* 2012; 287: 4503-4517.
- [29] van der Deen M, Taipaleenmäki H, Zhang Y, Teplyuk NM, Gupta A, Cinghu S, Shogren K, Maran A, Yaszemski MJ, Ling L, Cool SM, Leong DT, Dierkes C, Zustin J, Salto-Tellez M, Ito Y, Bae SC, Zielenska M, Squire JA, Lian JB, Stein JL, Zambetti GP, Jones SN, Galindo M, Hesse E, Stein GS, Van Wijnen AJ. MicroRNA-34c inversely couples the biological functions of the runt-related transcription factor RUNX2 and the tumor suppressor p53 in osteosarcoma. *J Biol Chem* 2013; 288: 21307-21319.
- [30] Lucero CM, Vega OA, Osorio MM, Tapia JC, Antonelli M, Stein GS, van Wijnen AJ, Galindo MA. The cancer-related transcription factor Runx2 modulates cell proliferation in human osteosarcoma cell lines. *J Cell Physiol* 2013; 228: 714-723.
- [31] Rowse GJ, Ritland SR, Gendler SJ. Genetic modulation of neu proto-oncogene-induced mammary tumorigenesis. *Cancer Res* 1998; 58: 2675-2679.
- [32] Davie SA, Maglione JE, Manner CK, Young D, Cardiff RD, MacLeod CL, Ellies LG. Effects of FVB/NJ and C57Bl/6J strain backgrounds on mammary tumor phenotype in inducible nitric oxide synthase deficient mice. *Transgenic Res* 2007; 16: 193-201.
- [33] Strien J, Sanft J, Mall G. Enhancement of PCR amplification of moderate GC-containing and highly GC-rich DNA sequences. *Mol Biotechnol* 2013; 54: 1048-1054.
- [34] Jensen MA, Fukushima M, Davis RW. DMSO and betaine greatly improve amplification of GC-rich constructs in de novo synthesis. *PLoS One* 2010; 5: e11024.
- [35] Farrell EM, Alexandre G. Bovine serum albumin further enhances the effects of organic solvents on increased yield of polymerase chain reaction of GC-rich templates. *BMC Res Notes* 2012; 5: 257.
- [36] Benita Y, Oosting RS, Lok MC, Wise MJ, Humphery-Smith I. Regionalized GC content of template DNA as a predictor of PCR success. *Nucleic Acids Res* 2003; 31: e99.
- [37] Lund AH, van Lohuizen M. RUNX: a trilogy of cancer genes. *Cancer Cell* 2002; 1: 213-215.
- [38] Nathan SS, Huvos AG, Casas-Ganem JE, Yang R, Linkov I, Sowers R, DiResta GR, Gorlick R, Healey JH. Tumour interstitial fluid pressure may regulate angiogenic factors in osteosarcoma. *Ann Acad Med Singapore* 2009; 38: 1041-1047.
- [39] Del Mare S, Kurek KC, Stein GS, Lian JB, Aqeilan RI. Role of the WWOX tumor suppressor gene in bone homeostasis and the pathogenesis of osteosarcoma. *Am J Cancer Res* 2011; 1: 585-594.
- [40] de Andrea CE, Petrilli AS, Jesus-Garcia R, Bleggi-Torres LF, Alves MT. Large and round tumor nuclei in osteosarcoma: good outcome. *Int J Clin Exp Pathol* 2011; 4: 169-174.